Iranian Journal of Chemical Engineering
Vol. 16, No. 3 (Summer 2019), IAChE

Nelder-Mead Algorithm Optimization and Galerkin's Method for Thermal Performance Analysis of Circular Porous Fins with Various Profiles in Fully Wet Conditions

M. R. Talaghat*[*], *F. Shafiei

Department of Chemical, Petroleum & Gas Engineering, Shiraz University of Technology, Shiraz, Iran

ARTICLE INFO

Article history:
Received: 2019-05-08
Accepted: 2019-10-23

Keywords:
Circular Porous Fins,
Relative Humidity,
Efficiency,
Effectiveness,
Optimization,
Galerkin Method

ABSTRACT

The main objective of this research is to analyze optimization and the thermal performance of circular porous fins with four different profiles, rectangular, convex, triangular, and concave under fully wet conditions. In this research, a linear model was used for the relationship between humidity and temperature. Moreover, modeling was assumed one-dimensional and the temperature changed only in the direction of the radius of the fin. Moreover, the thermal conductivity and heat transfer coefficient were a function of porosity and temperature, respectively. The governing equations were solved using Galerkin's method, the finite difference method, and the Gauss-Seidel algorithm. In this study, the effects of different parameters including relative humidity, Darcy number, Rayleigh number and porosity on temperature distribution, fin efficiency, and fin effectiveness were investigated. The results showed that the efficiency and effectiveness and heat transfer rate to the base for the rectangular profile were higher than those of other profiles. In this research, the Nelder-Mead algorithm was used for optimization. The results showed that to maintain optimal conditions, the ratio of thickness to fin length should be increased by increasing relative humidity or decreasing the Darcy number, Rayleigh number, and porosity.

1. Introduction

Fins or extended surfaces are used in many industrial applications such as air conditioning, refrigeration, and chemical processing systems [1]. In cooling and dehumidification processes, heat and mass transfer occurs simultaneously when the coil surface temperature is below the dew point temperature of the cooled air. If the temperature on the fin surface is higher than the ambiance dew point temperature, only sensible heat transfers from the air to fin. In this case, the fin is fully dry. If the temperature of the total fin surface is lower than the dew point, it produces both sensible and latent heat and that fin exists in a fully wet condition. The fin is called partially wet when the base temperature is lower than the dew point of air and the tip temperature is higher than the dew point [2, 3]. Many studies

[*]Corresponding author: talaghat@sutech.ac.ir

have been carried out to obtain the efficiency and effectiveness of the fin.

McQuiston [4] provided analytically the overall efficiency of a fully wet straight fin. He assumed that the driving force for the mass transfer was linearly related to the corresponding temperature difference. Wu and Bong [5] studied an analytical solution for the efficiency of a straight fin under both fully wet and partially wet conditions. They used the temperature and humidity ratio differences as the driving forces for heat and mass transfer. They assumed that a linear relationship was between the humidity ratio of the saturated air on the fin surface and its temperature. Their studies showed that fin efficiency did not change with increasing or decreasing relative humidity. The optimum dimensions of annular fins of the trapezoidal profile with variable thermal conductivity and heat transfer coefficient were computed by Razelos and Imre [6]. They obtained their results for three materials of copper, aluminum, and carbon steel. Kim et al. [7] investigated the relationships between flow and heat transfer for a porous fin in a plate-fin heat exchanger with laboratory studies. Their laboratory studies were performed based on forced heat transfer conditions.

Kiwan and Al-Nimr [8] applied the concept of applying porous fins to enhance heat transfer. The main purpose of using porous fins is to increase the effective surface area of heat transfer to the ambient fluid. Kundu and Das [9] investigated performance analysis and optimization of straight conical fins. In this study, the fins were used with three main geometries: longitudinal, spinal, and annular. They assumed that the thermal conductivity of the fin was constant; however, the heat transfer coefficient was variable. Campus [10] studied high conductivity permeable fins and recognized that porous fins prepared a much higher rate of heat transfer than traditional fins. One-dimensional optimization of circular fins with uniform thickness was discussed in the study of Arslanturk [11]. He achieved two correlation equations that express the maximum heat transfer rate when the fin volume was taken as fixed. Naphon [12] numerically studied the heat transfer characteristics of the circular fin under dry surface, partially wet surface, and fully wet surface conditions. They investigated the effect of various parameters such as inside and outside Biot number, hot fluid temperature, cold fluid temperature, relative humidity, half fin pitch, and fin thickness on the dimensionless temperature distribution. Their results showed that different parameters affected the dimensionless temperature distribution. As these parameters increase or decrease, the dimensionless temperature changes. For example, as the inside Biot number and fin thickness increase, dimensional temperature increases. However, increasing the outside Biot number, half fin pinch, relative humidity, and hot and cold fluid temperatures decreased dimensionless temperature. Sharqawy and Zubair [13] investigated the efficiency and optimization of an annular fin by considering heat and mass transfer. They obtained differential equations analytically for an annular fin in fully wet conditions.

Kiwan [14] investigated the thermal analysis of natural convection in a porous fin. He solved his governing equations using the fourth-order Runge-Kutta method. In this research, he studied three types of fins including infinite fin and non-insulated tips. Gorla and Bakier [15] achieved the thermal analysis of natural convection and radiation in porous fins. They solved the governing

equations using the fourth-order Runge–Kutta method. Then, they investigated three types of fins: the longfin, insulated tip, finite length fin with a known convective coefficient at the tip. Kundu and Bhanja [16] studied the effect of different parameters on the distribution of temperature, efficiency, and effectiveness of the rectangular porous fin. They also predicted the maximum heat transfer rate. Moradi [17] studied the heat transfer in a porous triangular fin with temperature-dependent thermal conductivity in the presence of convection and radiation heat transfer. In this study, mathematical modeling was solved by the differential transformation method (DTM), and its results were compared with numerical results.

Darvishi et al. [18] studied natural convection and radiation in a radial porous fin with variable thermal conductivity. Darvishi et al. [19] studied the thermal performance of a porous radial fin with natural convection and radiative heat losses. Sobamowo [20] studied heat transfer in a porous fin with temperature-dependent thermal conductivity and internal heat generation using Legendre wavelet collocation method. Jooma and Harley [21] studied heat transfer modeling in a radial fin. They proposed a time-dependent nonlinear differential equation for heat transfer in this fin. Daradji and Bouaziz [22] studied the modeling of a spiral porous fin. In this research, they studied the thermal conductivity coefficient both independently of temperature and through a linear relationship with temperature. Alhumoud [23] studied the problem of conjugate natural convection flow in a layer of porous media confined by two vertical thermally conductive surfaces. In this research, the effects of the wall thermal conductivity parameter, fluid and porous interfacial convective heat transfer parameter, and the Rayleigh number on the thermal behavior of the cavity are studied and analyzed.

The main purpose of this research is to supply a numerical solution (Gauss-Seidel method) and an analytical solution (Galerkin's Method) for the temperature distribution, efficiency and effectiveness of circular porous fins under the fully wet condition by applying the temperature and humidity ratio differences as the driving forces for heat and mass transfer systems, respectively.

2. Mathematical formulation

A physical model of the circular porous fins with variable sections is shown in Fig. (1).

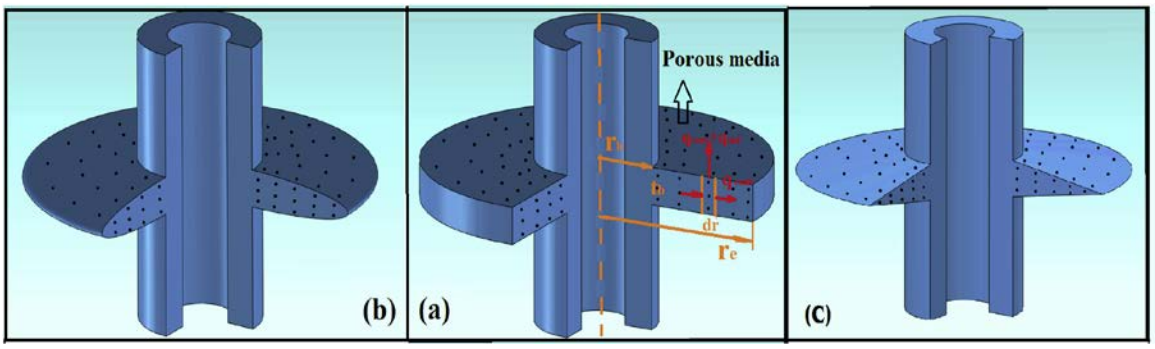

Figure 1. Schematics of fully wet circular porous fins: a) rectangular section, b) convex section, and c) triangular section.

The following assumptions are made to solve this problem [15-17, 24-26].

1. The thermal conductivity is a function of porosity.
2. Heat transfer coefficient is a function of temperature.
3. Condensation latent heat of the water vapor is assumed to be constant.
4. The moist airflow is steady with uniform velocities.
5. The thermal resistance related to the presence of water film due to condensation is low and negligible.
6. The effect of air pressure drop due to airflow is neglected.
7. There is no bond resistance in the fin base, and there are no heat sources in the fin itself.
8. Fin base temperature is constant.
9. The surface radiant exchanges are neglected.
10. No temperature variation across the fin thickness is considered.
11. The interactions between the porous medium and the clear fluid can be simulated by the Darcy formulation.
12. The porous medium is homogenous, isotropic, and saturated with a single-phase fluid.
13. The temperature variation through the fin is one-dimensional.
14. All the physical properties of the fin and fluid are taken to be constant except that there is variation in the density of fluid that may affect the buoyancy term.
15. There are steady-state conditions.

Because of the above-mentioned assumptions, the energy equation gives:

$$q_r - q_{r+dr} = 2\left(2\pi rhdr\left(1-\varphi\right)\left(T-T_a\right) + 2\pi rh_D i_{fg}\left(1-\varphi\right)\left(\omega-\omega_a\right)dr + \dot{m}c_p\left(T-T_a\right)\right) \quad (1)$$

The first term on the right-hand side of Eq. 1 relates to the heat transfer from the fluid passing through the porous media to the fin surface. The second term in this equation reports the heat transfer between the ambient air and the fin due to the relative humidity in the ambient air. Moreover, Coefficient '2' mentioned in the above equation indicates the upper and lower fin surfaces.

The mass flow rate of the fluid passing through the porous material can be written as in the following equation:

$$\dot{m} = \rho \cdot \upsilon \cdot A = \rho \cdot \upsilon \cdot 2 \cdot \pi \cdot r \cdot dr \quad (2)$$

According to Darcy's model, the fluid velocity through the fins is obtained through Eq. (3) [15]:

$$\upsilon = \frac{gK\beta\left(T-T_a\right)}{\gamma} \quad (3)$$

Substituting Eqs. (2) and (3) into Eq. (1) leads to:

$$-\frac{dq}{dr} = 2\left(2\pi rh\left(1-\varphi\right)\left(T-T_a\right) + 2\pi rh_D i_{fg}\left(1-\varphi\right)\left(\omega-\omega_a\right) + 2\pi r\rho c_p \frac{gK\beta\left(T-T_a\right)}{\gamma}\left(T-T_a\right)\right) \quad (4)$$

Moreover, from Fourier's Law of heat conduction [25]:

$$q = -k_{eff} A \frac{dT}{dr} \quad (5)$$

k_{eff} can be defined through Eq. (6) [27]:

$$k_{eff} = \varphi k_f + \left(1-\varphi\right)k_s \quad (6)$$

Substituting Eq. (5) into Eq. (4) yields:

$$\frac{1}{r}\frac{d}{dr}\left(rt\left(r\right)\frac{dT}{dr}\right)=\frac{2h\left(1-\varphi\right)}{k_{eff}}\left(T-T_a\right)+\frac{2h_D i_{fg}\left(1-\varphi\right)}{k_{eff}}\left(\omega-\omega_a\right)+\frac{2\rho c_p gK\beta}{\gamma k_{eff}}\left(T-T_a\right)^2 \quad (7)$$

h can be defined in the following equation [28]:

$$h=h_a\left[\frac{T-T_a}{T_b-T_a}\right] \quad (8)$$

Based on the Chilton-Colburn analogy [29], the relation between the convection transfer heat transfer coefficient and the convection mass transfer coefficient is expressed in Eq. (9):

$$\frac{h}{h_D}=c_p Le^{\frac{2}{3}} \quad (9)$$

where Le is the Lewis number.

By substituting Eq. (9) into Eq. (7), Eq. (10) is obtained:

$$\frac{1}{r}\frac{d}{dr}\left(rt\left(r\right)\frac{dT}{dr}\right)=\frac{2h_a\left(1-\varphi\right)}{\left(T_b-T_a\right)k_{eff}}\left(T-T_a\right)^2+\frac{2h_a i_{fg}\left(1-\varphi\right)}{c_p Le^{\frac{2}{3}}k_{eff}}\left[\frac{T-T_a}{T_b-T_a}\right]\left(\omega-\omega_a\right)+\frac{2\rho c_p gK\beta}{\gamma k_{eff}}\left(T-T_a\right)^2 \quad (10)$$

Sharqawy and Zubair [1] assumed that there is a linear relationship between temperature and humidity over the temperature range $T_b \le T \le T_{dp}$:

$$\omega=a_2+b_2T \quad (11)$$

where

$$a_2=\omega_b-\frac{\omega_{dp}-\omega_b}{T_{dp}-T_b}T_b \quad (12)$$

$$b_2=\frac{\omega_{dp}-\omega_b}{T_{dp}-T_b} \quad (13)$$

By defining the following dimensionless parameters (Eq. 14) and thickness function $t\left(r\right)$ (Eq. 15) for different shapes in Fig. 1 [27] and their substitution in Eq. (10), the dimensionless temperature distribution is expressed through Eq. (16).

$$R=\frac{r-r_b}{r_e-r_b},\ \theta=\frac{T}{T_b},\ \theta_a=\frac{T_a}{T_b} \quad (14)$$

$$t\left(r\right)=t_b\left(\frac{r_e-r}{r_b-r}\right)^n=t_b\left(1-R\right)^n \quad (15)$$

where n is the shape factor and defined for three sections as follows: the rectangular section $\left(n=0\right)$, the convex section (n=0.5), and the triangular section $\left(n=1\right)$.

$$\left(1-R\right)^n\frac{d^2\theta}{dR^2}+\frac{L}{RL+r_b}\left(1-R\right)^n\frac{d\theta}{dR}-n\left(1-R\right)^{n-1}\frac{d\theta}{dR}=\frac{2h_a\left(1-\varphi\right)L^2}{\left(1-\theta_a\right)t_b k_{eff}}\left(\theta-\theta_a\right)^2+\frac{2h_a i_{fg}\left(1-\varphi\right)L^2 b_2}{t_b c_p Le^{\frac{2}{3}}k_{eff}\left(1-\theta_a\right)}\left(\theta-\theta_a\right)^2+\frac{2h_a i_{fg}\left(1-\varphi\right)\left(b_2T+a_2-\omega_a\right)L^2}{t_b c_p Le^{\frac{2}{3}}k_{eff}\left(1-\theta_a\right)T_b}\left(\theta-\theta_a\right)+\frac{2\rho c_p gK\beta L^2T_b}{t_b\gamma k_{eff}}\left(\theta-\theta_a\right)^2 \quad (16)$$

The parameters of Eq. (16) are defined as follows [27]:

$$m_0=\sqrt{\frac{2h_a(1-\varphi)}{k_{eff}t_b}},\ \mathrm{B}=\frac{i_{fg}}{c_pLe^{2/3}},\ m_1^2=m_0^2(1+Bb_2),\ k_r=\frac{k_{eff}}{k_f},\ Da=\frac{K}{t_b^2},\ \mathrm{Ra}=\mathrm{Gr}\cdot\mathrm{Pr}$$
$$\mathrm{m}_2=\frac{b_2T_a+a_2-\omega_a}{T_b},\ m_3=\frac{2Da\cdot Ra}{k_r}\left(\frac{L}{t_b}\right)^2 \qquad (17)$$

Finally, the second-order differential energy equation for the fully wet-surface porous circular fin is summarized as follows:

$$(1-R)^n\frac{d^2\theta}{dR^2}+\frac{L}{RL+r_b}(1-R)^n\frac{d\theta}{dR}-n(1-R)^{n-1}\frac{d\theta}{dR}$$
$$-\frac{m_1^2L^2}{(1-\theta_a)}(\theta-\theta_a)^2-\frac{m_0^2Bm_2L^2}{(1-\theta_a)}(\theta-\theta_a)-m_3(\theta-\theta_a)^2=0 \qquad (18)$$

It should be noted that, in the above energy equation, when the fin is in a dry-surface condition, then the parameters of porosity, the Darcy number, and Raily number is zero ($\varphi=Da=Ra=0$). Further, when the fin is solid (non-porous), then a_2, b_2, ω_2, and B are zero. In this study, boundary conditions are defined as follows:

$$\theta(0)=1,\ \left(\frac{d\theta}{dR}\right)_{R=1}=0 \qquad (19)$$

The actual heat transfer rate through the porous fin is determined by using Fourier's law of heat conduction in the base.

$$q_{actual}=-k_{eff}\,2\pi r_bt_b.\frac{T_b}{L}\left(\frac{d\theta}{dR}\right)_{R=0} \qquad (20)$$

The ideal heat transfer rate of the porous fin is also obtained when the entire fin surface is maintained at the base temperature of the fin. This rate is calculated through Eq. (23) [16].

$$q_{ideal}=2\pi\left(r_e^2-r_b^2\right)\left(h(1-\varphi)(T_b-T_a)+h_Di_{fg}(1-\varphi)(\omega_b-\omega_a)+\frac{\rho c_pgK\beta}{\gamma}(T_b-T_a)^2\right) \qquad (21)$$

The heat transfer rate when no fin is attached to the same base area is calculated by the following equation [16].

The fin efficiency and fin effectiveness are defined by Eqs. (23) and (24), respectively:

$$q_{no\ fin}=2\pi r_bt_b\left(h(T_b-T_a)+h_Di_{fg}(\omega_b-\omega_a)\right) \qquad (22)$$

$$\eta=\frac{q_{actual}}{q_{ideal}}=\frac{\left(\frac{-2r_b}{r_e+r_b}\right)\left(\frac{d\theta}{dR}\right)_{R=0}}{m_1^2L^2(1-\theta_a)+m_0^2Bm_2L^2+m_3(1-\theta_a)^2} \qquad (23)$$

$$\varepsilon=\frac{q_{actual}}{q_{no\ fin}}=\frac{-2(1-\varphi)\left(\frac{d\theta}{dR}\right)_{R=0}}{m_1^2t_bL(1-\theta_a)+m_0^2Bm_2t_bL} \qquad (24)$$

With a good approximation, the results showed that the surface area as a rectangular section can be used for all other surfaces when the fin thickness is very thin.

2.1. Solving the governing equation using Galerkin's method

Galerkin's method is one of the weighted residual methods (WRM) whose purpose of this method is to minimize the residual function introduced to the nonlinear second-order ordinary differential equation [30-31]. Suppose that a linear differential operator D is performed on a function u to generate a function p:

$$D\left(u\left(x\right)\right)=p\left(x\right) \qquad (25)$$

It is supposed that u is approximated by a function $\tilde{u}$, which is a linear combination of basic functions selected from a linearly independent set. That is:

$$u\cong\tilde{u}=\sum_{i=1}^{n}c_i\varphi_i \qquad (26)$$

By replacing Eq. (26) into the differential operator D, the outcome of the operations mostly is not $p\left(x\right)$. Therefore, there will be an error or residual:

$$E\left(x\right)=R\left(x\right)=D\left(\tilde{u}\left(x\right)-p\left(x\right)\right)\neq 0 \qquad (27)$$

The concept in Galerkin's Method is to force the residual to zero in some average sense over the domain. Hence,

$$\int_x R\left(x\right)W_i\left(x\right)dx=0 \qquad (28)$$
$$i=1,2,...,n$$

The number of weight functions (W_i) is exactly equal to that of coefficients (c_i). Finally, a set of algebraic equations (including n equation) for unknown coefficients c_i is obtained.

Galerkin's method may be viewed as a modification of the Least Squares Method. Rather than using the derivative of the residual for the unknown c_i, the derivative of the approximating function is used [31].

Some of the nonlinear second-order ordinary differential equations are not solved by an exact solution. Hence, Galerkin's method is used to solve the equation. Therefore, in this research, Galerkin's method is used to solve the governing equation. Here, to achieve the solution of the differential equation, the following six steps should be followed [26]:

Step 1:

Consider the residual function,

$$Risidual\ function\ =E\left(R\right)=R(R)=\left(1-R\right)^n\frac{d^2\theta}{dR^2}+\frac{L}{RL+r_b}\left(1-R\right)^n\frac{d\theta}{dR}-$$
$$n\left(1-R\right)^{n-1}\frac{d\theta}{dR}-\frac{m_1^2L^2}{\left(1-\theta_a\right)}\left(\theta-\theta_a\right)^2-m_2\left(\theta-\theta_a\right)^2 \qquad (29)$$

Step 2:

The trial function, which satisfies the boundary conditions, is assumed as follows:

$$Trial\ function\ =\theta\left(R\right)=1+c_1\left(R-\frac{R^2}{2}\right)+c_2\left(R-\frac{R^3}{3}\right)+c_3\left(R-\frac{R^4}{4}\right)+c_4\left(R-\frac{R^5}{5}\right) \qquad (30)$$

Step 3:

Derived from the trial function and substituted into the residual function, we get:

$$R(R)=E(R)=(1-R)^n\left(c_1(-1)+c_2(-2R)+c_3\left(-3R^2\right)+c_4\left(-4R^3\right)\right)$$
$$+\frac{L}{RL+r_b}(1-R)^n\left(c_1(1-R)+c_2\left(1-R^2\right)+c_3\left(1-R^3\right)+c_4\left(1-R^4\right)\right)$$
$$-n(1-R)^{n-1}\left(c_1(1-R)+c_2\left(1-R^2\right)+c_3\left(1-R^3\right)+c_4\left(1-R^4\right)\right)$$
$$-\frac{m_1^2L^2}{(1-\theta_a)}\left(1+c_1\left(R-\frac{R^2}{2}\right)+c_2\left(R-\frac{R^3}{3}\right)+c_3\left(R-\frac{R^4}{4}\right)+c_4\left(R-\frac{R^5}{5}\right)-\theta_a\right)^2 \quad (31)$$
$$-m_2\left(1+c_1\left(R-\frac{R^2}{2}\right)+c_2\left(R-\frac{R^3}{3}\right)+c_3\left(R-\frac{R^4}{4}\right)+c_4\left(R-\frac{R^5}{5}\right)-\theta_a\right)^2$$

Step 4:

According to the trial function (θ(R)), the weighting functions W_1 to W_4 are defined as follows:

$$W_1(R)=\left(R-\frac{R^2}{2}\right), W_2(R)=\left(R-\frac{R^3}{3}\right), W_3(R)=\left(R-\frac{R^4}{4}\right), W_4(R)=\left(R-\frac{R^5}{5}\right) \quad (32)$$

Step 5:

Through Eq. (28), the coefficients c_1-c_4 are obtained by solving simultaneously the following equation:

$$\int_R R(R).W_1(R)\,dR=0$$
$$\int_R R(R).W_2(R)\,dR=0 \quad (33)$$
$$\int_R R(R).W_3(R)\,dR=0$$
$$\int_R R(R).W_4(R)\,dR=0$$

Step 6:

i. Find the coefficients c_1-c_4: when the surface temperature is higher than the air temperature:

By simultaneously solving the equations shown in Eq. (33) and computing the coefficients c_1-c_4, the trial functions for circular fins with different profiles are obtained as follows:

a) For the rectangular section:

$$\theta(R)=1-1.20733942R+2.44994795R^2-3.12543124R^3+2.24231452R^4 \quad (34)$$
$$-0.65822982R^5$$

b) For the convex section:

$$\theta(R)=1-1.14114691R+2.12202135R^2-2.60133716R^3+1.78323745R^4 \quad (35)$$
$$-0.48937525R^5$$

c) For the triangular section:

$$\theta(R)=1-1.07718524R+1.80408713R^2-2.04413429R^3+1.23917135R^4 \quad (36)$$
$$-0.27804274R^5$$

ii. Find the coefficients $c_1 - c_4$: when the air temperature is higher than the surface temperature

Similar to State (i), the trial functions for State (ii) are defined as follows:

a) For the rectangular section:

$$\theta(R) = 1 + 2.18525452R - 4.37113135R^2 + 5.63533741R^3 - 4.14038321R^4 + 1.25092713R^5 \quad (37)$$

b) For the convex section:

$$\theta(R) = 1 + 2.03992149R - 3.63137563R^2 + 4.35983963R^3 - 2.96862963R^4 + 0.80725287R^5 \quad (38)$$

c) For the triangular section:

$$\theta(R) = 1 + 1.93683743R - 3.12008852R^2 + 3.44263972R^3 - 1.97992751R^4 + 0.39054237R^5 \quad (39)$$

2.2. Solving the governing equation using finite difference method

In order to solve the temperature distribution equations in the porous fin in the fully wet condition, it is necessary to solve the temperature distribution equations on the surface of the fin. The finite difference method is used to solve them. The finite difference method is an approximate numerical method for solving differential equations. In this method, the object is first subdivided into a finite number of small elements and, then, the differential equations are rewritten discretely; finally, the differential equations resulting from the discretization form a multi-equation algebraic system. Various methods can be used to solve the algebraic equation system. One of the most commonly used methods for solving algebraic equations is the Gauss-Seidel method. The Gauss-Seidel method is the most common iterative numerical method used to solve the linear equation system. In this method, first, the temperature of each node is selected equal to the initial value and, then, is obtained by the large iteration of the correct value of the variables. Moreover, the equations are solved at the smallest difference in two successive iterations for the unknowns. In this research, MATLAB software is used to solve the equation system by the Gauss-Seidel iterative method [30].

2.3. Solving the governing equation for the fully wet porous fin

The dimensionless temperature distribution of a circular fin with the rectangular section in fully wet surface conditions is shown as in Eq. (40).

$$\frac{d^2\theta}{dR^2} + \frac{L}{RL + r_b}\frac{d\theta}{dR} - \frac{m_1^2 L^2}{(1-\theta_a)}(\theta - \theta_a)^2 - \frac{m_0^2 B m_2 L^2}{(1-\theta_a)}(\theta - \theta_a) - m_3(\theta - \theta_a)^2 = 0 \quad (40)$$

By using the definition of the finite difference method for the first- and second-order differential equations and placement in Equation (40), discrete Equation (41) is obtained:

$$\frac{(\theta_{i+1}-2\theta_i+\theta_{i-1})}{\Delta r^2}+\left(\frac{\theta_{i+1}-\theta_{i-1}}{2\Delta r}\right)\left(\frac{L}{RL+r_b}-1\right)$$
$$-(\theta_i-\theta_a)^2\left(\frac{m_1^2L^2}{(1-\theta_a)}-m_3\right)-(\theta_i-\theta_a)\left(\frac{m_0^2Bm_2L^2}{(1-\theta_a)}\right)=0 \quad (41)$$

Finally, for the middle nodes and the simple mathematical calculations, the temperature of each node is obtained through Eq. (42):

$$\theta_i=\frac{\left(\begin{array}{l}\theta_{i+1}\left(1+\left(\frac{L}{RL+r_b}\right)\left(\frac{\Delta R}{2}\right)\right)+\theta_{i-1}\left(1-\left(\frac{L}{RL+r_b}\right)\left(\frac{\Delta R}{2}\right)\right)\\-\left(\frac{m_1^2L^2\Delta R^2}{(1-\theta_a)}+m_3\Delta R^2\right)\theta_a{}^2+\left(\frac{m_0^2Bm_2L^2}{(1-\theta_a)}\right)\theta_a\Delta R^2\end{array}\right)}{\left(2+\left(\frac{m_1^2L^2}{(1-\theta_a)}+m_3\right)(\theta_i-2\theta_a)\Delta R^2+\frac{m_0^2Bm_2L^2}{(1-\theta_a)}\Delta R^2\right)} \quad (42)$$

2.4. Optimization analysis using the Nelder-Mead algorithm

Since the price of the developed surfaces depends on the type of the blade and its dimensions, the dimensions of the fins should be optimized [1, 13]. The goal of optimization of fins is to commonly determine the fin dimensions to either maximize the heat transfer rate for a specified fin volume or to minimize the fin volume for a specified heat transfer rate. Because the results of both approaches are the same, choosing each of these two approaches depends on the design specifications [26, 28, 32]. The volume of the fin and the dimensionless actual heat transfer rate is obtained through the following equations:

$$V=2\pi r_b t_b.L=0.02\left(m^3\right) \quad (43)$$

$$Q_{actual}=\frac{|q_{actual}|}{2\pi r_b.k_s.T_b}=\psi\xi\left(\frac{d\theta}{dR}\right)_{R=0} \quad (44)$$

where ψ and ξ are defined as follows:

$$\psi=\frac{t_b}{L},\xi=\frac{k_{eff}}{k_s} \quad (45)$$

It is necessary to be noticed that the volume of the fin for the rectangular, convex, and triangular profiles is calculated through Equation (43), because the thickness of the fin is very thin.

In this study, the objective function f with the following bounds is used to investigate the optimization of fins:

$$\text{Minimize: } f=-Q_{actual} \quad (46a)$$
$$\text{Subject to: } V=0.04\left(m^3\right) \text{ and } r_b=0.25(m) \quad (46b)$$

In this research, the Nelder-Mead optimization method is used for rectangular, convex, and triangular profiles; moreover, the maximum heat transfer rate is obtained

through Eq. (45), because the Nelder-Mead [33] algorithm is one of the best-known algorithms for multi-dimensional unconstrained optimization without derivatives.

3. Results and discussion

The main objective of this research is to investigate the temperature distribution and efficiency and effectiveness of circular porous fins under fully wet conditions. In this phenomenon, the temperature and humidity differences between the environment and the fin are the driving forces for heat and mass transfer, respectively. The numerical method (Gauss-Seidel method) and the analytical method (Galerkin method) have been used in this study. In this study, the reference values for calculations are presented in Table 1.

Moreover, necessary data for calculating a_2 and b_2 constants in Eq. (11) are extracted from CATT software (Computer-Aided Thermodynamics Tables). The results are shown in Table 2.

Table 1
The parameters used for validating this research [26].

$r_b = 0.1\,(\mathrm{m})$	Base temperature: T_b (°C)=50
$L = 0.4\,(\mathrm{m})$	Air temperature: T_a (°C)=30
Porosity $\varphi = 40\%$	Solid thermal conductivity: $k_s = 237\,(Wm^{-1}K^{-1})$
Darcy No.: Da=0.0001	Air heat transfer coefficient: $h_a = 25\,(Wm^{-2}K^{-1})$
Rayleigh No.: Ra=10000	Fluid thermal conductivity: $k_f = 0.0262\,(Wm^{-1}K^{-1})$
Lewis No.: $Le = 1$	Fin thickness: $t_b = 0.01\,(\mathrm{m})$

Table 2
The necessary data for calculating a_2 and b_2 constants from CAAT software.

RH (%)	T_a (°C)	ω_a	T_{dp} (°C)	ω_{dp}	T_b (°C)	ω_b
60	40	0.02843	30.74	0.02843	20	0.01469
80	40	0.0385	35.88	0.0385	20	0.01469
100	40	0.04888	40	0.04888	20	0.01469

To evaluate the model, the results of this modeling were compared with the data in the literature. The dimensionless temperature distribution for a fully wet circular porous fin with a rectangular section is demonstrated in Fig. 2. According to this figure, there is good agreement between the present work and the Hatami and Ganji's work [26]. Moreover, the results confirm the validity of this work.

Further, the dimensionless temperature distribution for a circular porous fin with various section types was calculated by the numerical (finite difference) and analytical methods (Galerkin's method). These results are demonstrated in Fig. 3 (a, b). As is clear from these figures, there is good agreement between the numerical method (using the finite difference method) and the analytical method (using Galerkin's method). Moreover, the results confirm the validity of this work.

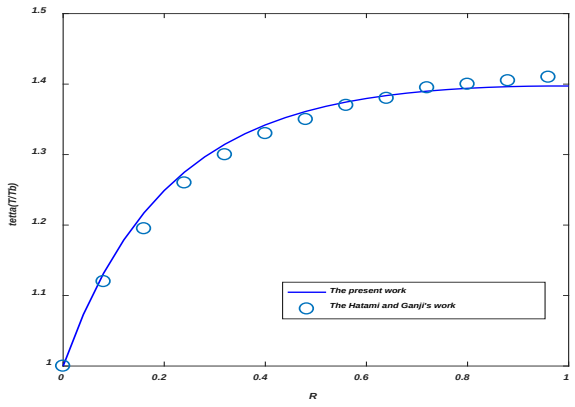

Figure 2. Comparison between results of this study and those obtained by Hatami and Ganji for the distribution of the temperature of a porous circular fin in a completely wet condition.

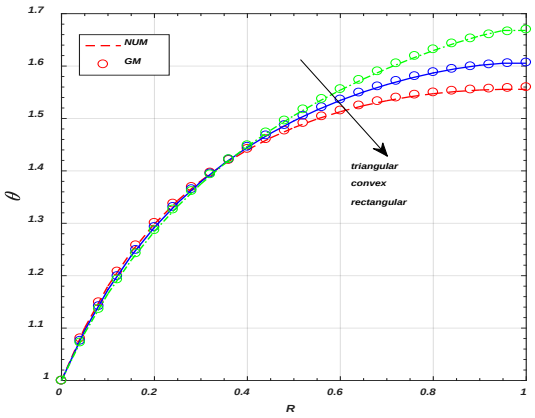

Figure 3a. Comparison of results of numerical solution by Galerkin's method for different section types when the air temperature is higher than the surface temperature.

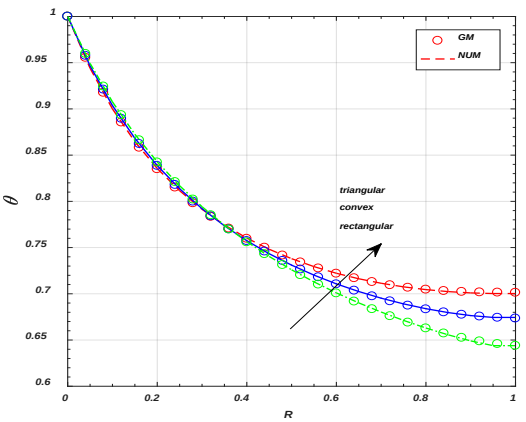

Figure 3b. Comparison of results of the numerical solution by Galerkin's method for different section types when the surface temperature is higher than the air temperature.

After assuring the accuracy of the model presented in this study, the effects of different parameters such as relative humidity, Darcy number, Raily number, and porosity on the distribution of temperature, efficiency, and effectiveness factors on the fully wet circular porous fin were studied. The results of this review are described below. Fig. 4 illustrates the effect of relative humidity on the distribution of dimensionless temperature. As is clear from this figure, when relative humidity increases, the dimensionless temperature increases. As a result of condensation, the latent heat of evaporation is released. This causes the fin temperature to rise.

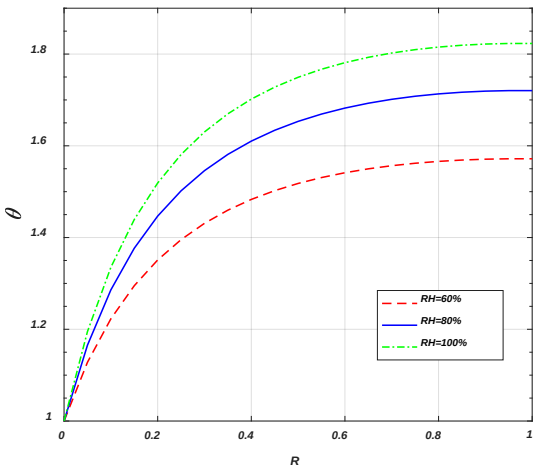

Figure 4. Effect of relative humidity on temperature distribution for the rectangular section fin.

The effect of Darcy number on the distribution of dimensionless temperature was studied. The results are shown in Fig. 5. According to the Darcy number definition, lowering the fin permeability reduces the Darcy number. This means that less fluid passes through the fin. Therefore, the collision between the fluid flow and the porous fin pores increases. Eventually, the surface temperature of the fin increases.

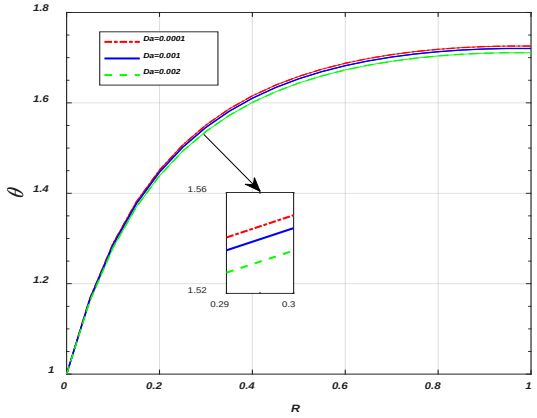

Figure 5. Effect of Darcy number on temperature distribution for the rectangular section fin.

Fig. 6 demonstrates the effect of Rayleigh number on the distribution of dimensionless temperature. Based on the defined Rayleigh number, as the buoyancy force decreases, the Rayleigh number decreases, too. When the rail number is reduced, the effective heat transfer convection coefficient between the fin and the surrounding air is reduced. As a result, the heat transfer rate is reduced. Reducing heat transfer causes the fin temperature to increase. Therefore, in practice, the ratio of thickness to fin length should be increased to reduce the Darcy number and provide optimal conditions.

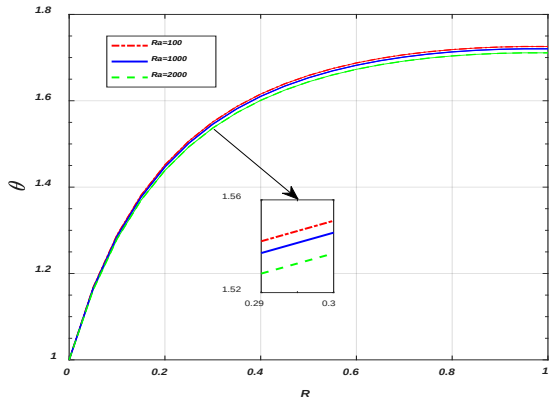

Figure 6. Effect of Rayleigh number on temperature distribution for the rectangular section fin.

In addition, the effect of porosity on the distribution of dimensionless temperature was studied. The results are presented in Fig. 7. As shown in this figure, as the porosity increases, the effective thermal conductivity decreases. As the fluid passes through the porous medium, the convection heat transfer coefficient decreases, resulting in a lower surface temperature. Further, in practice, the ratio of thickness to fin length should be increased to reduce the Rayleigh number and provide optimal conditions.

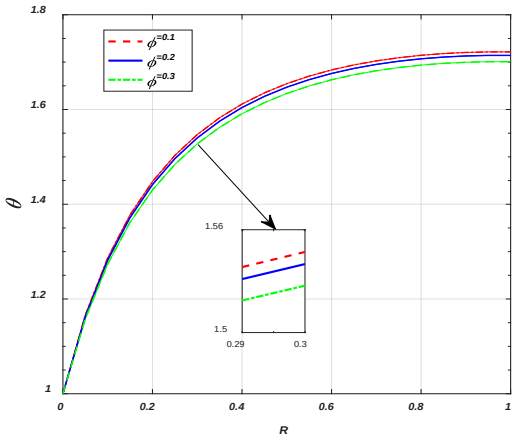

Figure 7. Effect of porosity on temperature distribution for the rectangular section fin.

Fig. 8 shows that relative humidity has a reverse effect on the efficiency of fins, i.e., with increasing the relative humidity, both the actual heat transfer rate and the ideal heat transfer rate increase (see Eq. (20)). In this case, the effect of the ideal heat transfer rate is greater than that of the actual heat transfer rate.

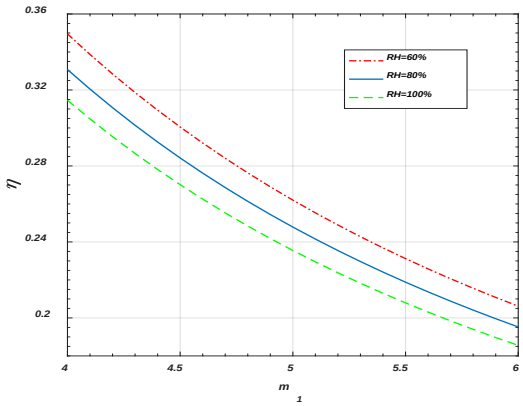

Figure 8. Effect of relative humidity on temperature distribution for the rectangular section fin.

As shown in Fig. 9, fin efficiency decreases with decreasing Darcy number, because both the actual and ideal heat transfer rates increase (see Eq. (20)). As a result, the fin efficiency can be reduced.

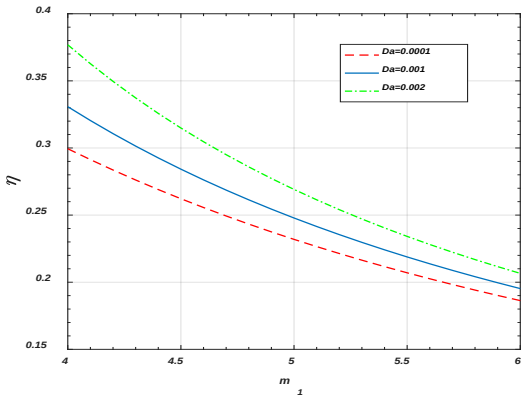

Figure 9. Effect of Darcy number on fin efficiency for the rectangular section fin.

Fig. 10 shows the effect of the rail number on the Finn efficiency. By reducing the rail number, fin efficiency decreases, because the actual heat transfer rate is lower than the ideal heat transfer rate.

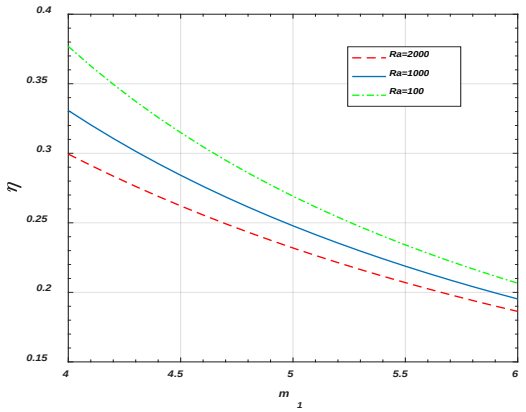

Figure 10. Effect of Rayleigh number on fin efficiency for the rectangular section fin.

Moreover, the effect of porosity on fin efficiency was studied. The results are shown in Fig. 11. As can be seen in this figure, the fin efficiency improves with increasing porosity of the fin. As the porosity increases, both the actual heat transfer rate and the ideal heat transfer rate are reduced (see Eq. (20)); however, the ideal heat transfer rate further decreases.

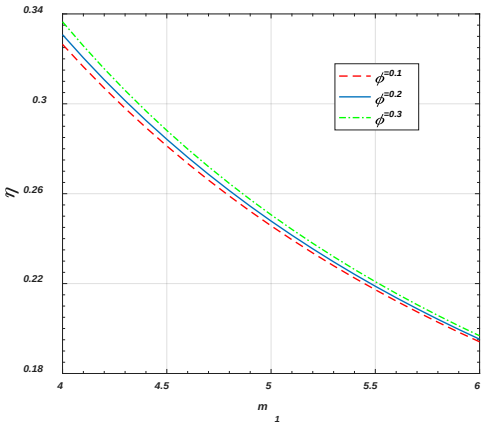

Figure 11. Effect of porosity on fin efficiency for the rectangular section fin.

Fig. 12 shows that relative humidity has a reverse effect on the effectiveness of the fin, i.e., increasing relative humidity increases both the actual heat transfer rate and the ideal heat transfer rate (see Eq. (21)), because the effect of the ideal heat transfer rate is greater than that of the actual heat transfer rate.

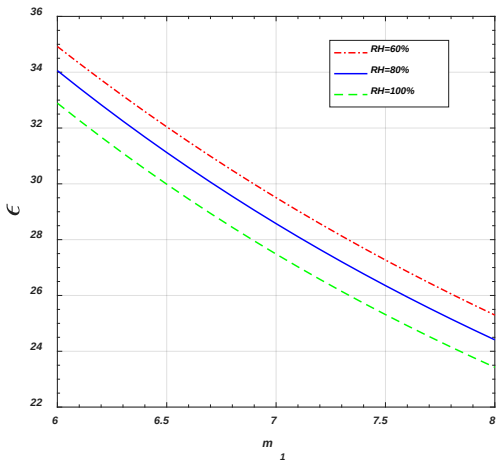

Figure 12. Effect of relative humidity on the fin effectiveness factor for the rectangular section fin.

As shown in Fig. 13, the fin effectiveness factor increases with decreasing Darcy number.

The actual heat transfer rate increases, but the heat transfer rate in the un-finned condition does not change according to Eq. (21), thus improving the efficiency of the fin.

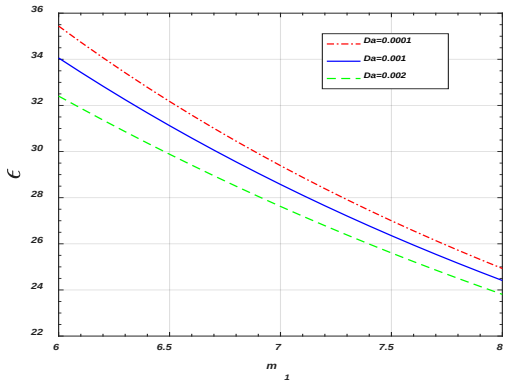

Figure 13. Effect of Darcy number on the fin effectiveness factor for the rectangular section fin.

Fig. 14 shows the effect of the Rayleigh number on the fin effectiveness factor. As shown in this figure, a decrease in the Rayleigh number increases the fin effectiveness factor.

As the Rayleigh number increases, the rate of heat transfer to the fin decreases. According to the definition of the fin effectiveness factor, the coefficient will decrease.

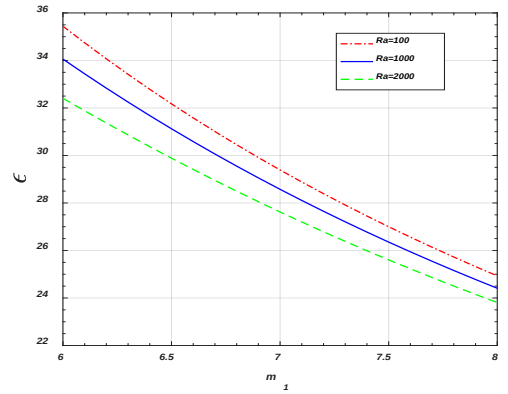

Figure 14. Effect of Rayleigh number on the fin effectiveness factor for the rectangular section fin.

Fig. 15 shows the effect of the porosity on the fin effectiveness factor. As can be seen in Fig. 15, the fin effectiveness decreases by increasing fin porosity. As the porosity increases, the actual heat transfer rate is reduced; however, the ideal heat transfer rate does not change (see Eq. (21)); in this case, the fin effectiveness is reduced.

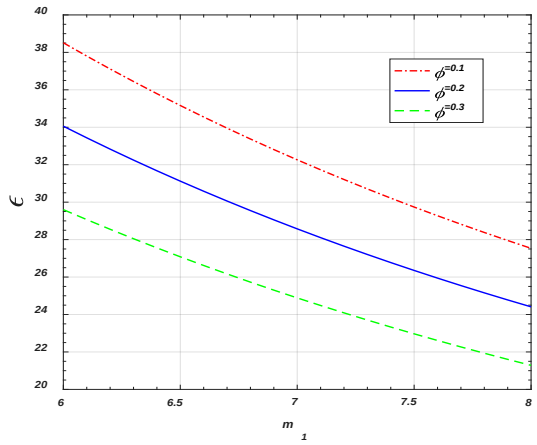

Figure15. Effect of porosity on the fin effectiveness factor for the rectangular section fin.

Further, in this research, optimum design analysis for the circular porous fin using the Nelder-Mead algorithm was carried out. Moreover, the effect of volume, relative humidity, Darcy number, Rayleigh number, and porosity on the optimum heat transfer rate was studied. The results are shown in Figs. 16 to 20. As shown in 16, by increasing volume, heat transfer in the porous circular fin with a rectangular section type is increased under fully wet conditions. It can also be concluded that when the volume increases, the optimal ratio of thickness to length increases. This means that the fin thickness should be increased or the fin length should be reduced.

Fig. 17 shows the effect of the relative humidity on the optimum heat transfer rate.

As shown in the figure, by increasing relative humidity, heat transfer in the porous circular fin with the rectangular section type is increased. As shown in Figs. 16 and 17, at a constant ratio of thickness to the length of the fin, the optimal dimensional transfer increases as the fin volume increases or the relative humidity increases. Therefore, to maintain optimum conditions, the thickness value must be increased relative to the fin length by increasing the dimensionless fin volume.

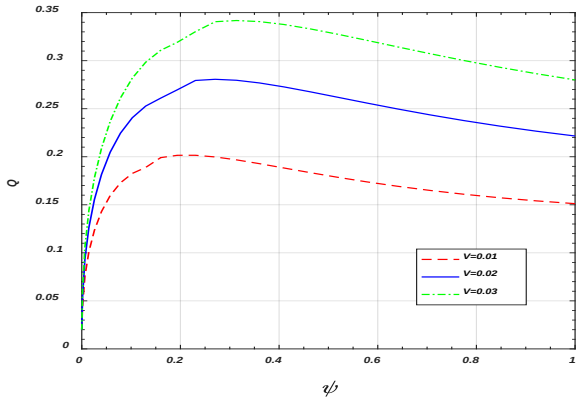

Figure 16. Effect of fin volume on the optimum heat transfer rate for the rectangular section fin.

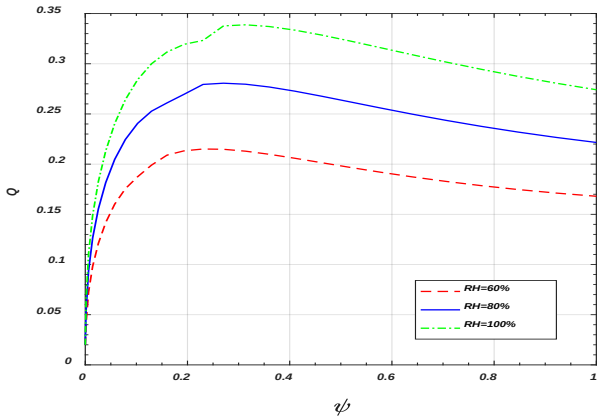

Figure 17. Effect of relative humidity on the optimum heat transfer rate for the rectangular section fin.

Reversely, as shown in Figs. 18 to 20, by increasing the Darcy number, Rayleigh number, and porosity, the dimensionless optimum heat transfer rate is decreased.

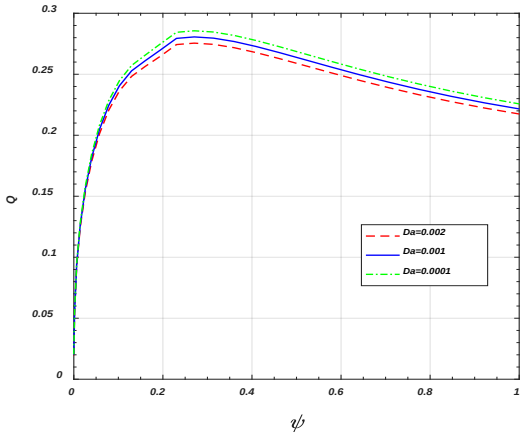

Figure 18. Effect of Darcy number on the optimum heat transfer rate for the rectangular section fin.

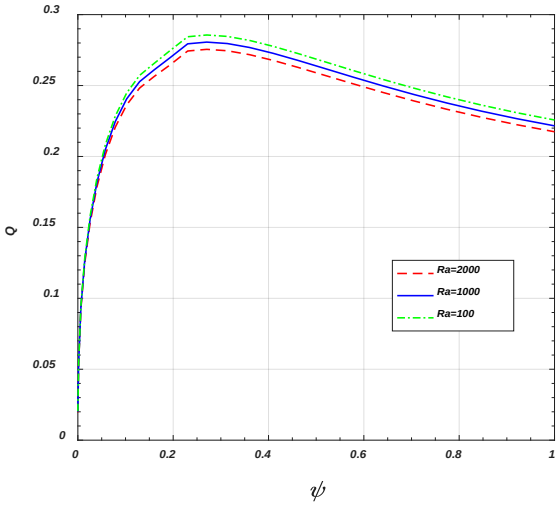

Figure 19. Effect of Rayleigh number on the optimum heat transfer rate for the rectangular section fin.

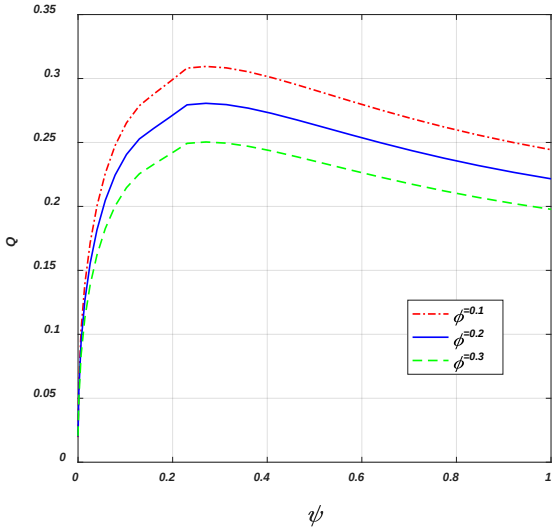

Figure 20. Effect of porosity on the optimum heat transfer rate for the rectangular section fin.

Finally, the temperature distribution, fin efficiency, effectiveness factor, and optimum heat transfer rate for the circular porous fin with various section types (including rectangular, convex, and triangular profiles) were studied. The results are shown in Figs. 21 to 24. The result showed that, in the same conditions, the efficiency and effectiveness factor of a circular porous fin with a rectangular section shape is greater than that of others.

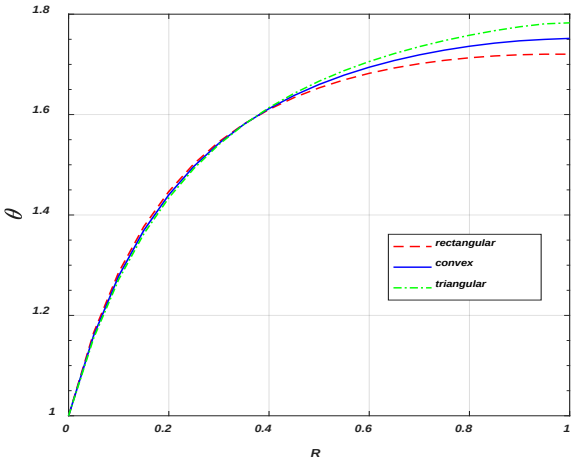

Figure 21. Effect of section profile types on temperature distribution.

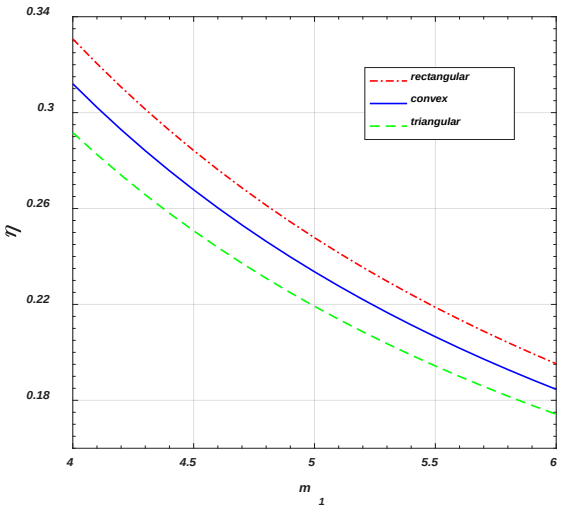

Figure 22. Effect of section profile types on fin efficiency.

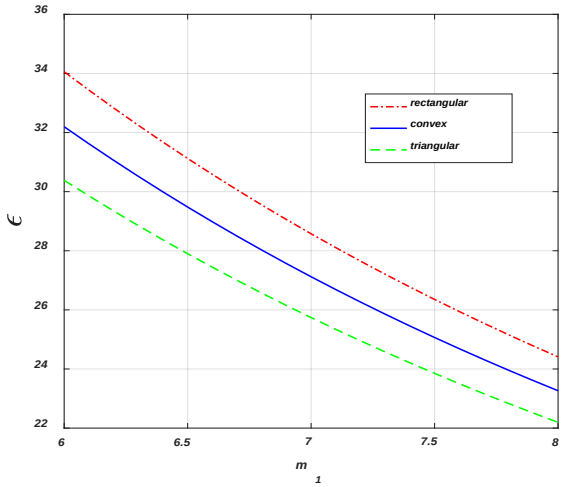

Figure 23. Effect of section profile types on fin effectiveness.

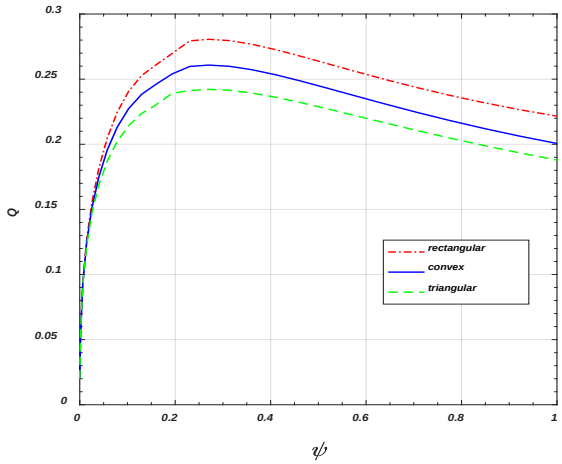

Figure 24. Effect of section profile types on optimum heat transfer rate.

4. Conclusions

In this paper, the temperature distribution, the thermal performance, and the optimum design analysis for the circular porous fin in fully wet conditions with four variable section shapes, namely rectangular, convex, triangular, and concave, using the Nelder-Mead algorithm were presented, and there was good agreement between the present numerical work, Galerkin's method, and Hatami and Ganji's work [26]. In this modeling, the temperature and humidity ratio differences are the driving forces for the heat and mass transfer, respectively. The following important points can be drawn from the present work:

1. The convergence of the dimensionless temperature distribution and the efficiency for a fully wet circular porous fin with the rectangular section was studied. The results confirmed the validity of this work.
2. If the relative humidity of the ambient air increased, the temperature increased; however, the efficiency and the effectiveness decreased.
3. The temperature distribution and fin's effectiveness were enhanced by declining the Darcy number and the Rayleigh number;

however, the fin's efficiency was reduced due to a decrease in the Darcy number and Rayleigh number.

4. The high porosity caused the fin surface temperature and the effectiveness of fin to decrease; moreover, the efficiency of fin increased.

5. At a constant value of the thickness-to-length ratio of the fin, by increasing the dimensionless fin volume per unit width, the magnitude of the dimensionless optimum heat transfer rate increased; therefore, with an increase in the dimensionless fin volume per unit width, the value of the thickness-to-length ratio of the fin needs to be increased to maintain the optimum condition.

6. The difference in temperature distribution at the end of the fin was higher. Moreover, the efficiency and effectiveness and heat transfer rate to the fin base for the rectangular section of the other forms were greater.

7. At a constant value of the thickness-to-length ratio of the fin, the magnitude of the dimensionless optimum heat transfer rate increased by increasing the relative humidity or decreasing the Darcy and Rayleigh numbers and porosity. Then, the value of the thickness-to-length ratio of the fin needs to be increased to maintain the optimum condition with an increase in the relative humidity or a decrease in the Darcy and Rayleigh numbers, and the same holds for porosity.

Nomenclature

A	cross section area of the fin [m^2].
c_i	coefficients for Eq. 26.
c_p	specific heat [J kg^{-1} K^{-1}].
Da	Darcy number.
E(R)	residual function.
f	objective function.
g	gravity [m s^{-2}].
h_a	constant in Eq. (8) [W m^{-2} K^{1}].
h	convection heat transfer coefficient [W m^{-2} K^{1}].
h_D	convection mass transfer coefficient.
i_{fg}	latent heat of water vaporization.
k	thermal conductivity [W m^{-1} K^{1}].
k_r	fluid thermal conductivity to solid thermal conductivity ratio, see Eq. (13).
K	permeability [m^2].
k_{eff}	effective thermal conductivity of fin [W m^{-1} K^{1}].
k_f	thermal conductivity of the fluid [W m^{-1} K^{1}].
k_s	solid thermal conductivity [W m^{-1} K^{1}].
m_1	dry fin constants defined in Eq. (13) [m^{-1}].
m_2	constant defined in Eq. (13).
$\dot{m}$	mass flow rate [kg s^{-1}].
n	thickness profile index.
q	actual heat transfer rate of the porous fin [W].
Q	dimensionless actual heat transfer rate.
R	dimensionless radius.
Ra	Rayleigh number.
r	radial direction.
r_b	fin base radius [m].
r_e	fin end radius [m].
R(R)	residual function.
S_H	porous parameter.
t_b	thickness at the fin base [m].
$t(r)$	thickness of the fin [m].
T	temperature [^{o}C].
T_b	fin base temperature [^{o}C].
T_{dp}	dew point temperature [^{o}C].
u	approximate function in Eq. 25.
V	volume [m^3].
W_i	weight function.

Greek symbols

β	coefficient of volumetric thermal expansion [K^{-1}].
ε	fin effectiveness.
η	fin efficiency.
ξ	effective thermal conductivity to

	solid thermal conductivity ratio, see Eq. (23).
ψ	base thickness to length ratio.
θ	dimensionless temperature.
$\theta(R)$	trial function.
υ	velocity of fluid passing through the fin [m s^{-1}].
γ	kinematic viscosity [m s^{-2}].
ρ	density [kg m^{-3}].
φ	porosity.
ω	relative humidity.
ω_a	ambient relative humidity.
ω_b	base fin humidity ratio.
ω_{dp}	humidity ratio at dew point temperature.

Subscripts

a	ambient condition.
b	base condition.
e	end condition.
f	fluid properties.
eff	porous properties.
s	solid properties.

References

[1] Sharqawy, M. H. and Zubair, S. M., "Efficiency and optimization of straight fins with combined heat and mass transfer–An analytical solution", *Applied Thermal Engineering*, **28** (17), 2279 (2008).

[2] Sabbaghi, S., Rezaii, A., Shahri, G. R. and Baktash, M., "Mathematical analysis for the efficiency of a semi-spherical fin with simultaneous heat and mass transfer", *International Journal of Refrigeration*, **34** (8), 1877 (2011).

[3] Hatami, M., Ahangar, G. R. M., Ganji, D. and Boubaker, K., "Refrigeration efficiency analysis for fully wet semi-spherical porous fins", *Energy Conversion and Management*, **84**, 533 (2014).

[4] McQuiston, F., "Fin efficiency with combined heat and mass transfer", *ASHRAE Transactions*, **81** (1), 350 (1975).

[5] Wu, G. and Bong, T. Y., "Overall efficiency of a straight fin with combined heat and mass transfer", *ASHRAE Transactions*, **100** (1), 367 (1994).

[6] Razelos, P. and Imre, K., "The optimum dimensions of circular fins with variable thermal parameters", *Journal of Heat Transfer*, **102** (3), 420 (1980).

[7] Kim, S. Paek, J. and Kang, B., "Flow and heat transfer correlations for porous fin in a plate-fin heat exchanger", *Journal of Heat Transfer*, **122** (3), 572 (2000).

[8] Kiwan, S. and Al-Nimr, M., "Using porous fins for heat transfer enhancement", *Journal of Heat Transfer*, **123** (4), 790 (2001).

[9] Kundu, B. and Das, P., "Performance analysis and optimization of straight taper fins with variable heat transfer coefficient", *International Journal of Heat and Mass Transfer*, **45** (24), 4739 (2002).

[10] Abu-Hijleh, B. A/K, "Natural convection heat transfer from a cylinder with high conductivity permeable fins", *Journal of Heat Transfer*, **125** (2), 282 (2003).

[11] Arslanturk, C., "Simple correlation equations for optimum design of annular fins with uniform thickness", *Applied Thermal Engineering*, **25** (14), 2463 (2005).

[12] Naphon, P., "Study on the heat transfer characteristics of the annular fin under dry-surface, partially wet-surface, and fully wet-surface conditions", *International Communications in Heat and Mass Transfer*, **33** (1), 112 (2006).

[13] Sharqawy, M. H. and Zubair, S. M., "Efficiency and optimization of an annular fin with combined heat and mass

transfer–An analytical solution", *International Journal of Refrigeration*, **30** (5), 751 (2007).

[14] Kiwan, S., "Thermal analysis of natural convection porous fins", *Transport in Porous Media*, **67** (1), 17 (2007).

[15] Gorla, R. S. R. and Bakier, A., "Thermal analysis of natural convection and radiation in porous fins", *International Communications in Heat and Mass Transfer*, **38** (5), 638 (2011).

[16] Kundu, B., Bhanja, D. and Lee, K. S., "A model on the basis of analytics for computing maximum heat transfer in porous fins", *International Journal of Heat and Mass Transfer*, **55** (25), 7611 (2012).

[17] Moradi, A., Hayat, T. and Alsaedi, A., "Convection-radiation thermal analysis of triangular porous fins with temperature-dependent thermal conductivity by dtm", *Energy Conversion and Management*, **77**, 70 (2014).

[18] Darvishi, M. T., Khani, F. and Gorla, R. S. R., "Natural convection and radiation in a radial porous fin with variable thermal conductivity", *International Journal of Applied Mechanics and Engineering*, **19** (1) 27 (2014).

[19] Darvishi, M. T., Gorla, R. S. R., Khani, F. and Aziz, A., "Termal performance of a porous radial fin with natural convection and radiative heat losses", *Thermal Science*, **9** (2), 669 (2015).

[20] Sobamowo, M. G., "Heat transfer study in porous fin with temperature dependent thermal conductivity and internal heat generation using Legendre wavelet collocation method", *Communication in Mathematical Modeling and Applications*, **2** (3), 16 (2017).

[21] Jooma, R. and Harley, C., "Heat transfer in a porous radial fin: Analysis of numerically obtained solutions" *Advances in Mathematical Physics*, Article ID: 1658305, 20 pages, (2017). (https://doi.org/10.1155/2017/1658305).

[22] Daradji, N. and Bouaziz, M. N., "Modelling a spiral porous fin with temperature dependent and independent thermal conductivity", *International Journal of Applied Engineering Research*, **13** (7), 5522 (2018).

[23] Alhumoud, J. M., "Non-equilibrium natural convection flow through a porous medium", *Mathematical Modeling of Engineering Problems*, **6** (2), 136 (2019).

[24] Kiwan, S., "Effect of radiative losses on the heat transfer from porous fins", *International Journal of Thermal Sciences*, **46** (10), 1046 (2007).

[25] Vahabzadeh, A., Ganji, D. and Abbasi, M., "Analytical investigation of porous pin fins with variable section in fully-wet conditions", *Case Studies in Thermal Engineering*, **5**, 1 (2015).

[26] Hatami, M. and Ganji, D., "Investigation of refrigeration efficiency for fully wet circular porous fins with variable sections by combined heat and mass transfer analysis", *International Journal of Refrigeration*, **40**, 140 (2014).

[27] Nield, D. A. and Bejan, A., Convection in porous media, 3rd ed., Springer, USA, p. 121 (2006).

[28] Hazarika, S. A., Bhanja, D., Nath, S. and Kundu, B., "Geometric optimization and performance study of a constructal t-shaped fin under simultaneous heat and mass transfer", *Applied Thermal Engineering*, **109**, 162 (2016).

[29] Chilton, T. H. and Colburn, A. P., "Mass transfer (absorption) coefficients

prediction from data on heat transfer and fluid friction", *Industrial & Engineering Chemistry*, **26** (11), 1183 (1934).

[30] Grandin, H., Jr., Fundamentals of the finite element method, Macmillan Publishing Company, p. 50 (1986).

[31] Cicelia, J. E., "Solution of weighted residual problems by using Galerkin's method", *Indian Journal of Science and Technology*, **7** (3S), 52 (2014).

[32] Kundu, B. and Bhanja, D. "An analytical prediction for performance and optimum design analysis of porous fins", *International Journal of Refrigeration*, **34** (1), 337 (2011).

[33] Nelder, J. A. and Mead, R., "A simplex method for function minimization", *The Computer Journal*, **7** (4), 308 (1965).